A

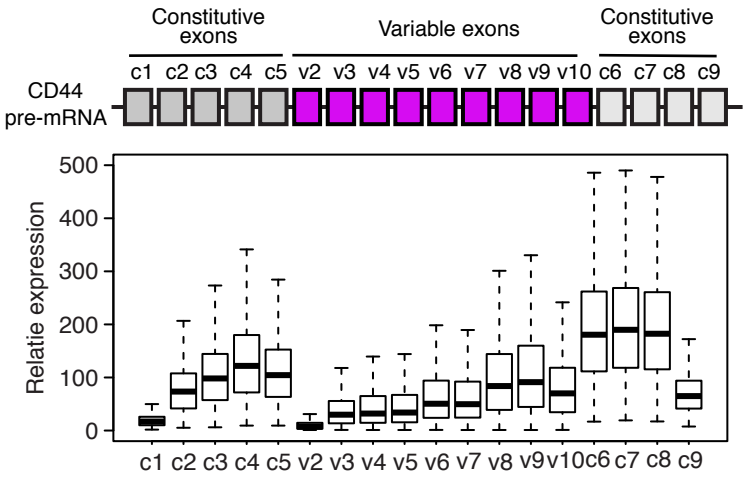
Constitutive exons
Variable exons
Constitutive exons
c1 c2 c3 c4 c5 v2 v3 v4 v5 v6 v7 v8 v9 v10 c6 c7 c8 c9
CD44 pre-mRNA
Relatie expression
500
400
300
200
100
0
c1 c2 c3 c4 c5 v2 v3 v4 v5 v6 v7 v8 v9 v10 c6 c7 c8 c9

B

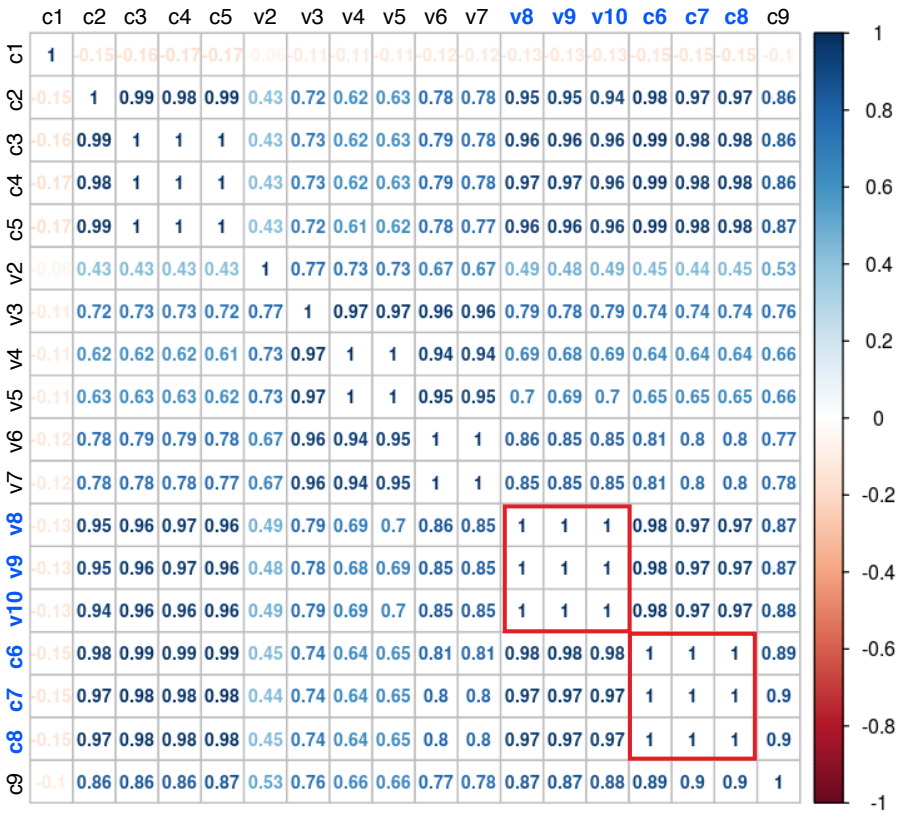
c1 c2 c3 c4 c5 v2 v3 v4 v5 v6 v7 v8 v9 v10 c6 c7 c8 c9
1
0.8
0.6
0.4
0.2
0
-0.2
-0.4
-0.6
-0.8
-1

C

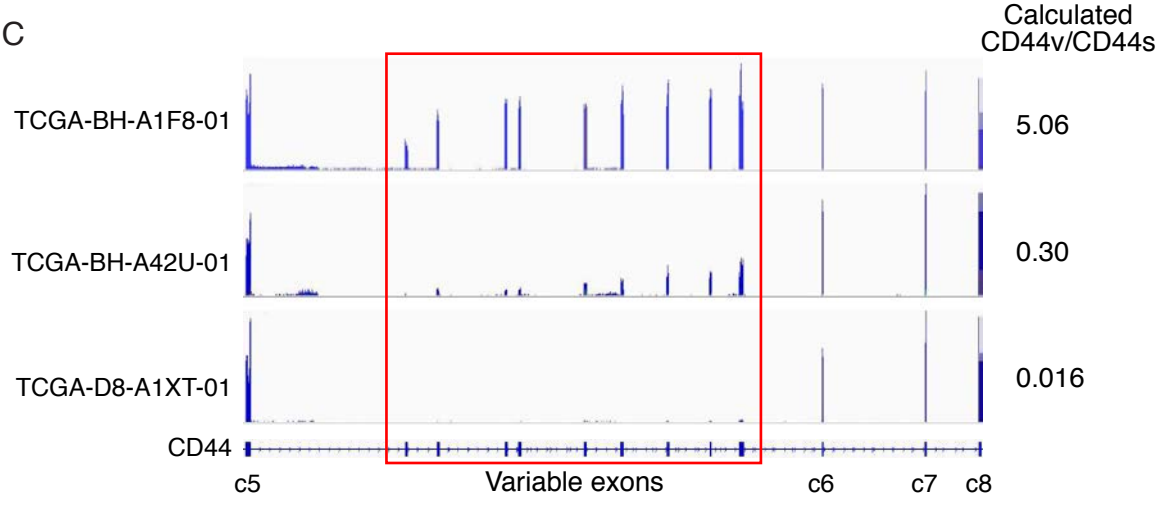
Calculated CD44v/CD44s
TCGA-BH-A1F8-01
5.06
TCGA-BH-A42U-01
0.30
TCGA-D8-A1XT-01
0.016
CD44
c5
Variable exons
c6
c7
c8

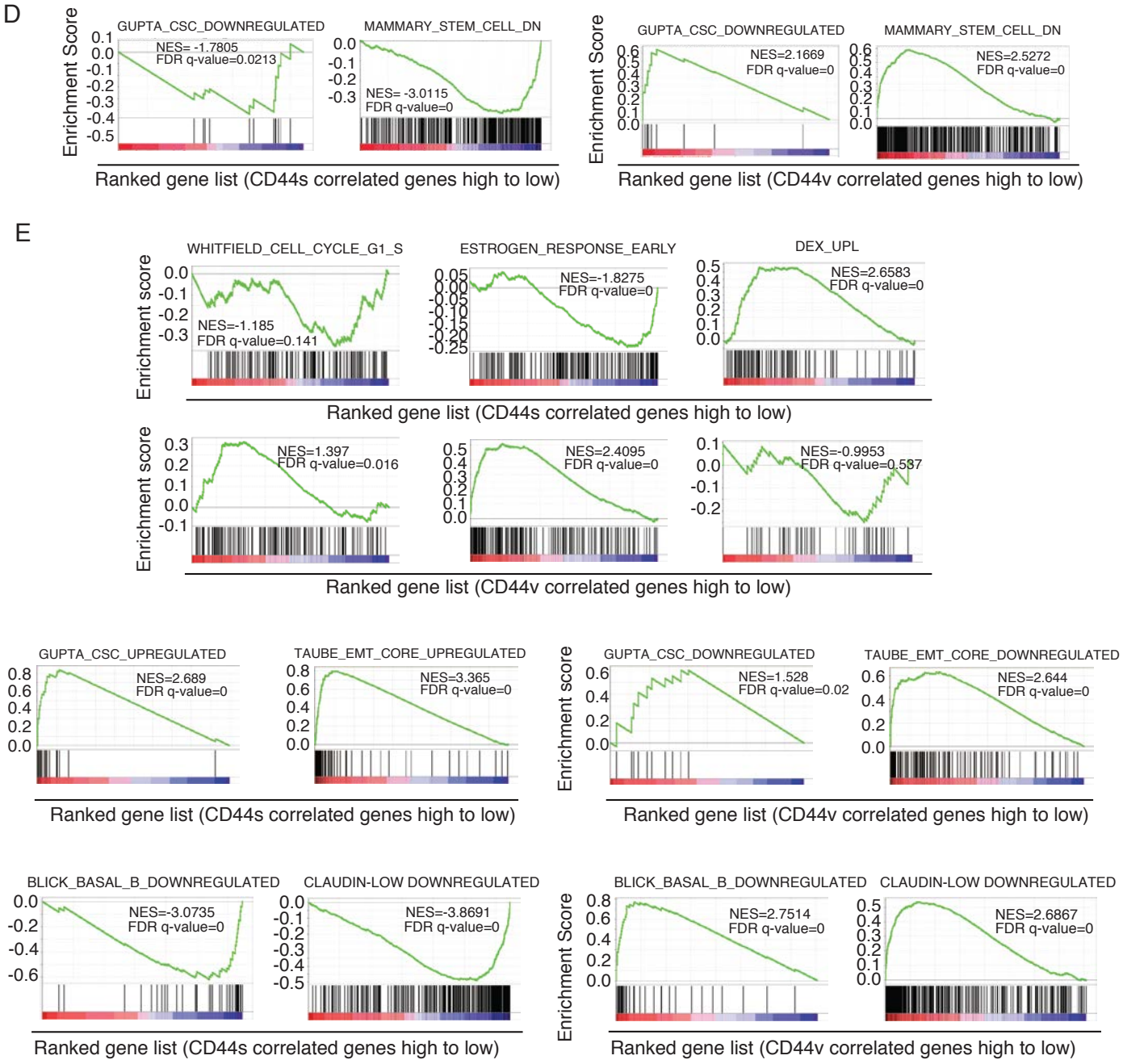

Figure S1. (A) Top, Diagram of human CD44 pre-mRNA depicting constitutive and variable exons. Bottom, CD44 exon expression in breast cancer patient TCGA dataset showing that exons v8, v9, and v10 were the most highly expressed variable exons, and exons c6,c7, and c8 were the most highly expressed constitutive exons. (B) Correlation of exon expression among different CD44 exons. Red boxes show the detected perfect correlations among v8, v9, and v10 or c6, c7, and c8. (C) IGV tracks showing CD44 reads distribution is in agreement with calculated CD44v to CD44s ratios. (D,E) GSEA of the Breat Cancer TCGA data showing inversed enrichments of CSC and mammary stem cell signatures (D), and G1-S, estrogene response early, and DEX_UPL gene signatures (E) in CD44s- and CD44v-correlated gene lists. (F) GSEA of the CCLE dataset showing the positive enrichment of CSC and EMT gene signatures in the CD44s-correlated gene list and negative enrichment in the CD44v-correlated gene list. (G) GSEA showing inversed enrichments of the Basal_B gene signature and Claudin_low signature in the CD44s- and CD44v-correlated gene list.

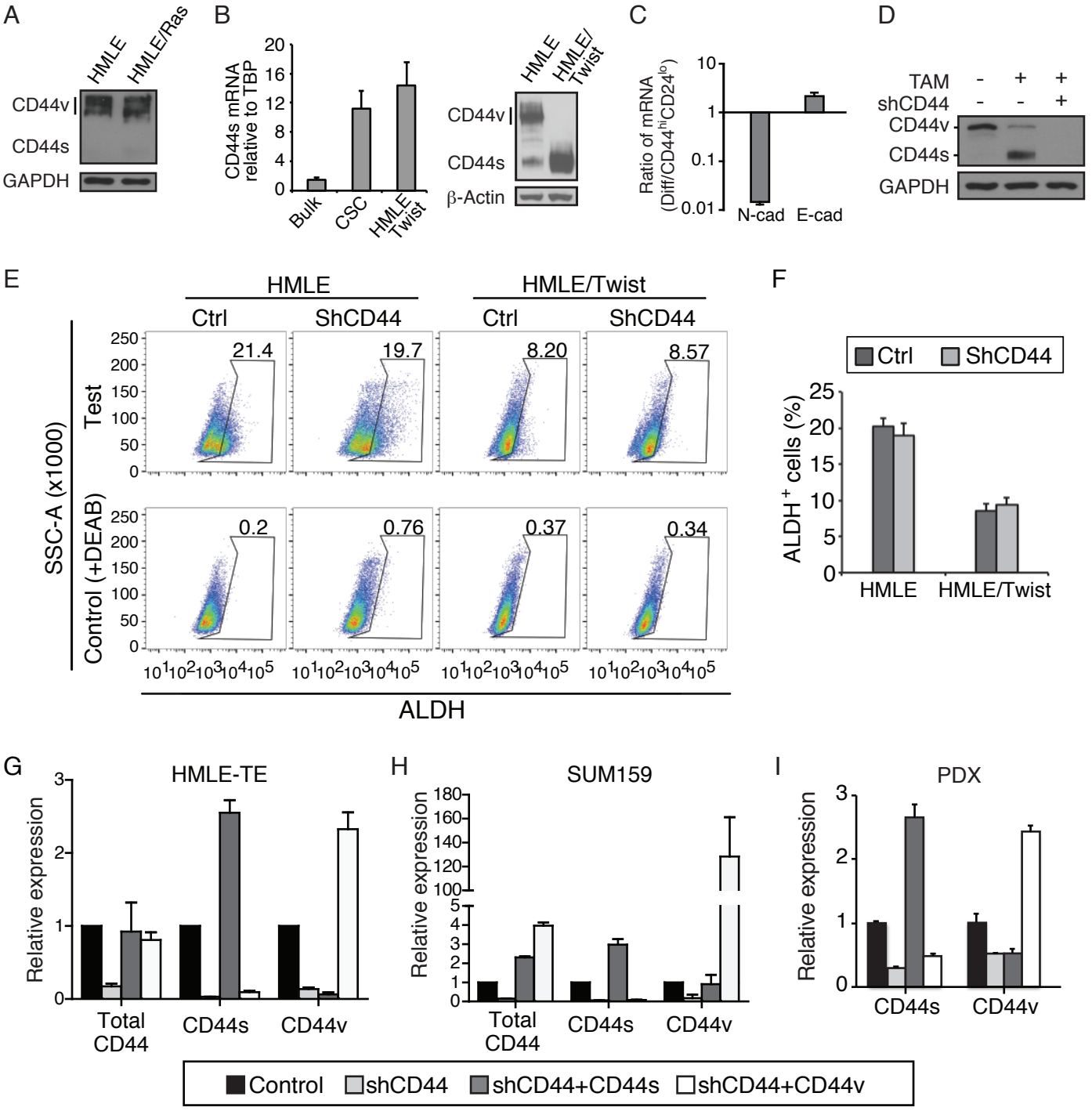

Figure S2. (A) Immunoblot of lysates from both HMLE and HMLE/Ras cells showing CD44v as the predominant isoform. The CD44v proteins ran in a cluster of bands due to post-translational modification of glycosylation. (B) Left Panel: mRNA levels of CD44s relative to TBP in Bulk, $CD44^{hi}/CD24^{lo}$ population of HMLE cells, and HMLE/Twist cells. Right Panel: Immunoblot of lysates from HMLE and HMLE/Twist cells. (C) The $CD44^{hi}/CD24^{lo}$ population of HMLE cells was grown in monolayer culture for 8 days. Relative mRNA levels of N-cadherin and E-cadherin at day 8 relative to day 0 are shown. (D) Immunoblot images showing the switch of CD44v to CD44s isoforms in TAM-treated HMLE/Twist-ER cells and knockdown efficiency of CD44 shRNA. (E,F) ALDH analysis in HMLE and HMLE/Twist cells that expressed control or CD44 shRNA. FACS images (E) and quantification of ALDH+ cells (F) are shown.(G-I) qRT-PCR results showing relative expression levels of CD44s and CD44v in tamoxifen treated HMLE/Twist-ER (HMLE-TE, G), SUM159 (H), and PDX tumor cells (I) that expressed CD44 shRNA or co-expressed CD44 shRNA and the CD44s or CD44v cDNA.

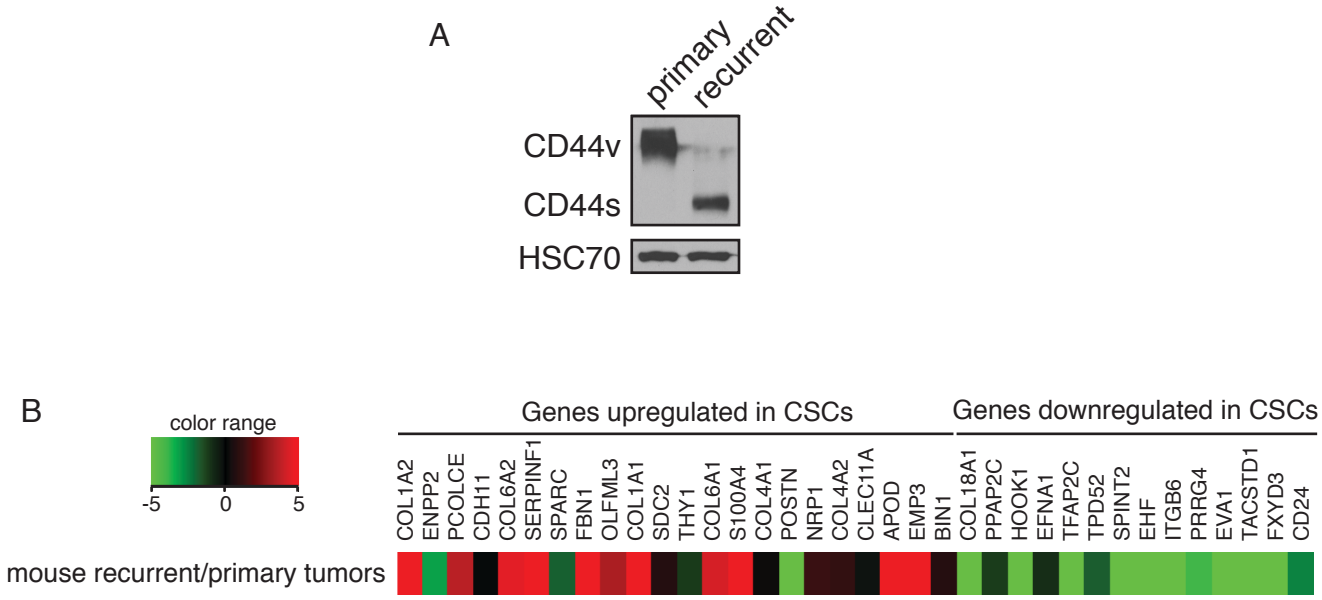

Figure S3. (A) Immunoblot images showing that CD44v is the predominant isoform in primary tumors and CD44s is the predominant isoform in recurrent tumors. (B) RNAs isolated from primary and recurrent breast tumors were analyzed by qRT-PCR for expression of the CSC signature. A heat plot of ratios of gene expression between recurrent and primary tumors is shown.

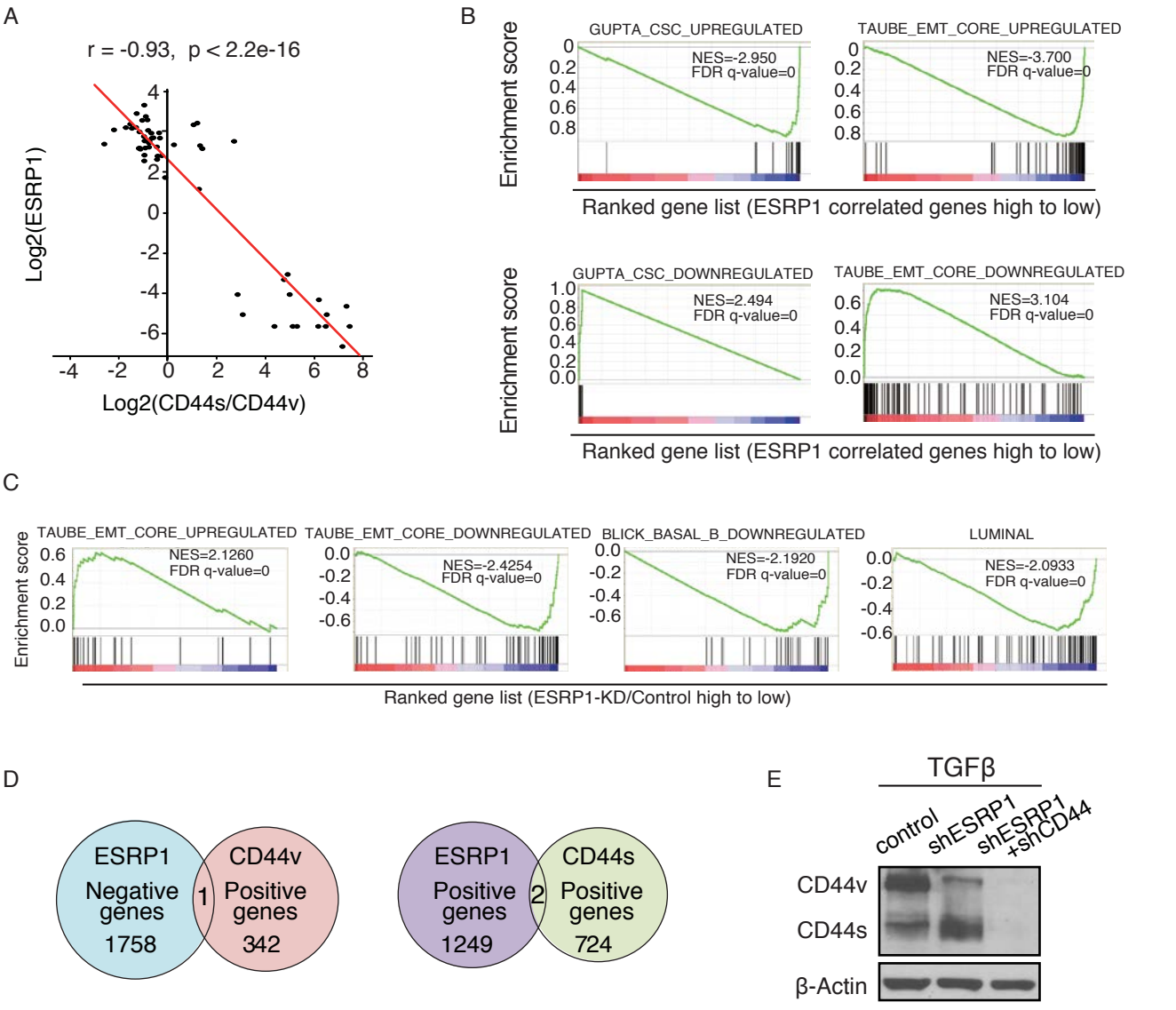

Figure S4. (A) Inverse correlation was shown between ESRP1 levels and the ratios of CD44s to CD44v using the CCLE Breast Cancer Cell line dataset. Log2 values are plotted. (B) CCLE data analysis showing that the ESRP1 gene signature negatively correlated with the CSC and EMT gene signatures. (C) GSEA analyses showing the positive enrichment of EMT signature and negative enrichment in Basal-downregulated and Lumina subtype upon ESRP1 silencing. (D) Venn diagram plots showing the overlapping of ESRP1-, CD44v-, and CD44s-associated genes using the breast cancer TCGA dataset. (E) Immunoblot images showing expression levels of CD44s and CD44v in TGFβ-treated control HMLE cells or cells that expressed ESRP1 shRNA or both ESRP1 and CD44 shRNAs.

A

CD44s Correlated Genes Ontology Analysis

Category	Term	P-Value
GOTERM_BP_FAT	response to wounding	2.10E-23
GOTERM_BP_FAT	regulation of programmed cell death	9.90E-12
GOTERM_BP_FAT	cell adhesion	2.80E-07
GOTERM_BP_FAT	regulation of cell proliferation	8.00E-07
GOTERM_BP_FAT	protein kinase cascade	5.30E-06
GOTERM_BP_FAT	cell surface receptor linked signal transduction	5.60E-06
GOTERM_BP_FAT	positive regulation of response to external stimulus	1.30E-04
GOTERM_BP_FAT	positive regulation of cell communication	2.20E-04
GOTERM_BP_FAT	cell migration	1.70E-03
GOTERM_BP_FAT	cell motility	3.40E-03

B

CD44v Correlated Genes Ontology Analysis

Category	Term	P-Value
GOTERM_BP_FAT	cell morphogenesis	4.00E-03
GOTERM_BP_FAT	biological adhesion	4.80E-03
GOTERM_BP_FAT	cell adhesion	4.90E-03
GOTERM_BP_FAT	cell-cell adhesion	7.60E-03
GOTERM_BP_FAT	cellular component morphogenesis	1.10E-02
GOTERM_BP_FAT	epithelial tube morphogenesis	4.10E-02

C

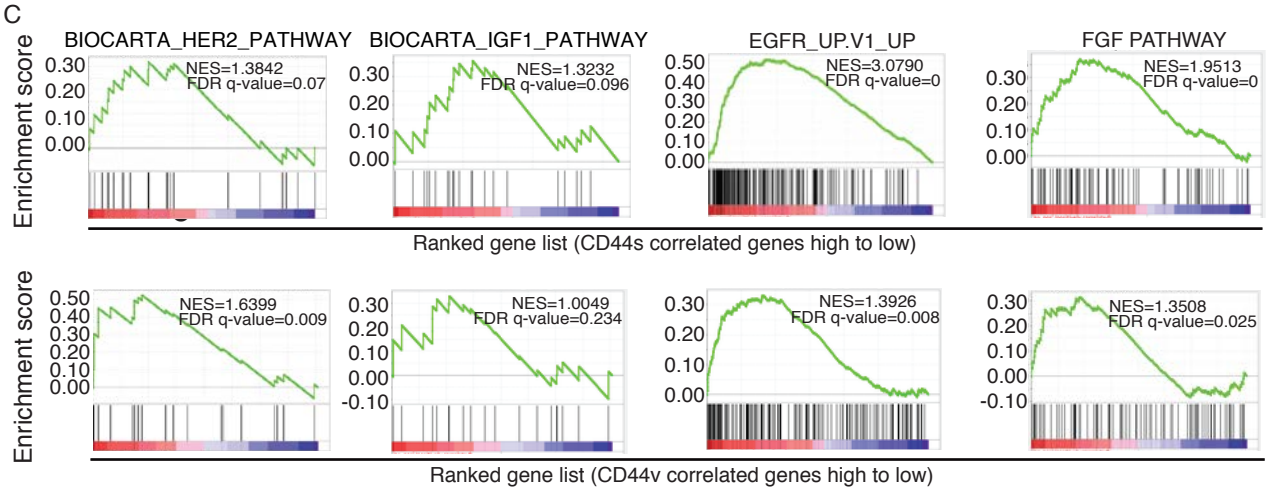

D

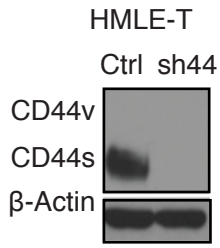

E

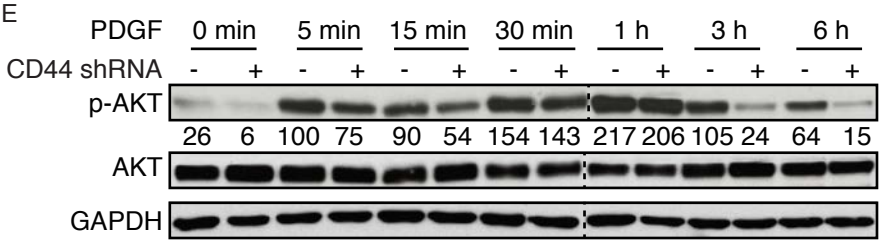

F

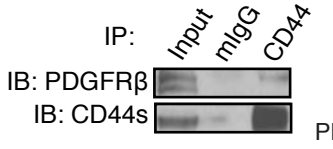

G

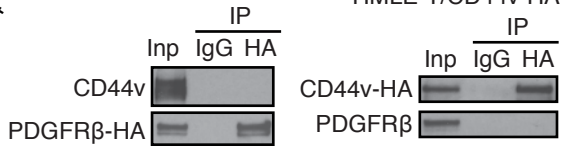

H

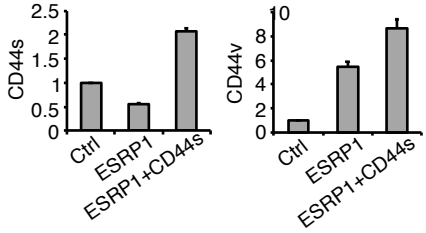

Figure S5. (A) Gene Ontology analysis of CD44s-correlated genes. (B) Gene Ontology analysis of CD44v-correlated genes. (C) GSEA analysis of HER2, IGF1, EGFR, and FGF pathway gene signatures in the CD44s- and CD44v-correlated gene lists. (D) Immunoblot images showing expression levels of CD44s and CD44v in HMLE-Twist (HMLE-T) cells that expressed control or CD44 shRNA. (E) Immunoblot of p-AKT, AKT and GAPDH in HMLE-Twist control and shCD44 cells. Cells were treated with PDGF(10 ng/ml) for the indicated time intervals. Relative intensity of phosphorylated to unphosphorylated AKT signals is depicted underneath of the images. (F) 293FT cells co-transfected with CD44s and FLAG-tagged PDGFRβ were subjected to CD44 immunoprecipitation (IP). (G) Co-immuniprecipitation (IP) experiments showing undetactable interaction between CD44v and PDGFRβ. PDGFRβ-HA cDNA or CD44v-HA cDNA was ectopically expressed in HMLE or HMLE-Twist cells, respectively. The co-IP was performed using an HA antibody and blotted for HA or CD44v or PDGFRβ as indicated. (H) Relative mRNA levels of CD44s and CD44v in HMLE/Twist cells that expressed ESRP1 cDNA or both ESRP1 and CD44s CDNA compared to control HMLE/Twist cells.

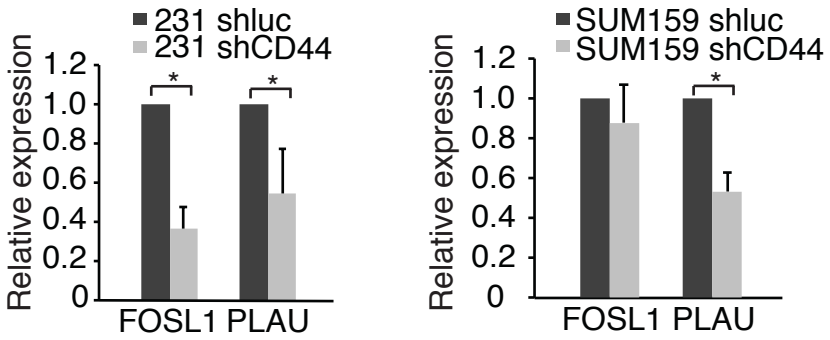

Figure S6. qRT-PCR showing relative expression levels of FOSL1 and PLAU in MDA-MB-231 cells (control and shCD44) and SUM159 cells (control and shCD44). Error bars indicates SEM. * $P < 0.05$.

SUPPLEMENTAL METHOD

Bioinformatics analyses of CD44 splice isoforms and associated biological pathways

The TCGA breast invasive carcinoma (BRCA) exon expression dataset by RNAseq (polyA+ IlluminaHiSeq) was downloaded from UCSC cancer browser. This cancer browser is now replaced by a new platform UCSC Xena browser (https://xenabrowser.net/datapages/).

The exon expression dataset measures the expression levels of individual exons in RPKM (Reads Per Kilobase of exon model per Million mapped reads). In theory, different exons in the same transcript isoform are expected to have the same RPKM expression values. However, two factors can impact exon expression levels. It has been observed that longer exons show relatively lower expression values. Therefore, the most 5' and 3' exons, which are usually larger-size exons compared to internal exons, show relative lower RPKM values. With this consideration, we excluded the use of 5' and 3' exons. Moreover, polyA-primed reverse transcription was used as a RNA-seq platform. This sequencing method resulted in a gradual decline of sequencing coverage from 3' to 5'. Thus, exons located at the 3' end were preferential considered when calculating isoform expression levels.

Fig. S1A depicts the CD44 exon structure. CD44v is composed of a family of CD44 mRNA that includes at least one of the nine variable exons. CD44s, on the other hand, is devoid of all variable exons. Our analysis of the more than 1000 specimens in the BRCA-TCGA dataset shows that v8, v9, v10 exons are almost always among the highest expressed CD44 variable exons (Fig. S1A) and are most highly correlated with each other (Fig. S1B). This observation is consistent with the structure of CD44v where these three variable exons are included in most of the CD44v isoforms, including CD44v3-10, CD44v6-10, and CD44v8-10 (1, 2). Likewise, constitutive exons c6, c7, c8 show highest expression and are mostly highly correlated (Fig. S1A, bottom panel). These constitutive exons also locate adjacent to v8-v10 exons. Thus, these results led us to use the average exon expression levels of v8, v9, v10 to represent CD44v and the average expression levels of c6, c7, c8 for total CD44. We used linear expression levels to calculate the levels of CD44v and total CD44. We then performed subtraction between total CD44 and CD44v to obtain levels of CD44s.

To determine the biological traits that are associated with CD44 splice isoforms, we performed GSEA analysis. We extracted CD44 isoform-associated gene lists by performing correlation analysis of CD44 isoform expression to the whole transcriptome. The correlation to CD44 splice isoforms was used to pre-rank the gene list and to perform GSEA analysis (3, 4). In addition to utilizing the signatures from the C2 and C5 collections in MsigDB (http://software.broadinstitute.org/gsea/msigdb/index.jsp), we utilized several of our own curated signatures. These signatures were derived from published literatures, including gene expression profiles of mouse MaSC and luminal progenitor enriched population use either Lin-/CD24/CD29 profiles (5, 6) and human CSC signatures originated studies (7-10).

For splicing factor analysis, splicing factors were extracted from Gene Ontology Consortium terms GO:0000380 and GO:0043484. Gene expression of these factors was downloaded from TCGA database. Correlation of each splicing factor to the ratio of CD44s/CD44v was measured using Pearson correlation coefficient. Splicing factors with absolute

Pearson correlation coefficient > 0.3 and P-value (Permuation test, randomly shuffled 100,000 times) < 10-6 were selected.

REFERENCES:

1. Ponta, H., Sherman, L., and Herrlich, P.A. 2003. CD44: from adhesion molecules to signalling regulators. *Nat Rev Mol Cell Biol* 4:33-45.
2. Zoller, M. 2011. CD44: can a cancer-initiating cell profit from an abundantly expressed molecule? *Nat Rev Cancer* 11:254-267.
3. Mootha, V.K., Lindgren, C.M., Eriksson, K.F., Subramanian, A., Sihag, S., Lehar, J., Puigserver, P., Carlsson, E., Ridderstrale, M., Laurila, E., et al. 2003. PGC-1alpha-responsive genes involved in oxidative phosphorylation are coordinately downregulated in human diabetes. *Nat Genet* 34:267-273.
4. Subramanian, A., Tamayo, P., Mootha, V.K., Mukherjee, S., Ebert, B.L., Gillette, M.A., Paulovich, A., Pomeroy, S.L., Golub, T.R., Lander, E.S., et al. 2005. Gene set enrichment analysis: a knowledge-based approach for interpreting genome-wide expression profiles. *Proc Natl Acad Sci U S A* 102:15545-15550.
5. Chakrabarti, R., Wei, Y., Hwang, J., Hang, X., Andres Blanco, M., Choudhury, A., Tiede, B., Romano, R.A., DeCoste, C., Mercatali, L., et al. 2014. DeltaNp63 promotes stem cell activity in mammary gland development and basal-like breast cancer by enhancing Fzd7 expression and Wnt signalling. *Nat Cell Biol* 16:1004-1015, 1001-1013.
6. Asselin-Labat, M.L., Vaillant, F., Sheridan, J.M., Pal, B., Wu, D., Simpson, E.R., Yasuda, H., Smyth, G.K., Martin, T.J., Lindeman, G.J., et al. 2010. Control of mammary stem cell function by steroid hormone signalling. *Nature* 465:798-802.
7. Blick, T., Hugo, H., Widodo, E., Waltham, M., Pinto, C., Mani, S.A., Weinberg, R.A., Neve, R.M., Lenburg, M.E., and Thompson, E.W. 2010. Epithelial mesenchymal transition traits in human breast cancer cell lines parallel the CD44(hi/)CD24 (lo/-) stem cell phenotype in human breast cancer. *J Mammary Gland Biol Neoplasia* 15:235-252.
8. Gupta, P.B., Onder, T.T., Jiang, G., Tao, K., Kuperwasser, C., Weinberg, R.A., and Lander, E.S. 2009. Identification of selective inhibitors of cancer stem cells by high-throughput screening. *Cell* 138:645-659.
9. Taube, J.H., Herschkowitz, J.I., Komurov, K., Zhou, A.Y., Gupta, S., Yang, J., Hartwell, K., Onder, T.T., Gupta, P.B., Evans, K.W., et al. 2010. Core epithelial-to-mesenchymal transition interactome gene-expression signature is associated with claudin-low and metaplastic breast cancer subtypes. *Proc Natl Acad Sci U S A* 107:15449-15454.
10. Hennessy, B.T., Gonzalez-Angulo, A.M., Stemke-Hale, K., Gilcrease, M.Z., Krishnamurthy, S., Lee, J.S., Fridlyand, J., Sahin, A., Agarwal, R., Joy, C., et al. 2009. Characterization of a naturally occurring breast cancer subset enriched in epithelial-to-mesenchymal transition and stem cell characteristics. *Cancer Res* 69:4116-4124.

Table S1

CD44s correlated gene list			**CD44v correlated gene list**	
Gene Name	Correlation		Gene Name	Correlation
CD44	0.872447058		CD44	0.99749632
TLR8	0.436266094		TRPS1	0.40683844
MPEG1	0.433311524		TCF20	0.36857307
MSN	0.419633489		AFTPH	0.36565682
PDCD1LG2	0.411900595		TLR5	0.36506708
CSF2RB	0.403358739		IRF6	0.36472871
PLEK	0.40196431		SLC1A2	0.36237749
RPS6KA1	0.400750847		VTCN1	0.36066084
SERPINB8	0.394588253		VDR	0.35906801
C1orf204	0.393248766		RCAN3	0.3586608
LRRC8C	0.391253568		TTLL1	0.35815741
IL10RA	0.391036241		BSPRY	0.35651686
LYN	0.390369145		CLCN3	0.355839
PTAFR	0.388993691		NIPAL3	0.35412812
SRGN	0.388616026		TARBP1	0.35393086
CYTH4	0.387994489		B3GNT2	0.35295607
DOK2	0.387023945		SLK	0.35293466
SIRPB2	0.384623272		ENAH	0.35218226
CD40	0.382275563		TMEM26	0.3511772
CD97	0.381967555		LOC10012853	0.34956747
TAGAP	0.381638486		MAP3K7	0.34743409
SOD2	0.381601567		TNK1	0.34389328
CSF1R	0.381259077		RASEF	0.34219578
CD14	0.381244952		KIF13A	0.34211773
CD53	0.380248474		LDLRAD3	0.341623
CCR5	0.379689344		STAT3	0.34018355
CD4	0.379323838		DLG1	0.34010802
TNFAIP8	0.379051868		SYT7	0.34004117
FGL2	0.378673267		WDR31	0.33927819
CXorf21	0.378291815		ZNF185	0.33758925
SNX20	0.378215855		PRRG4	0.33751009
FGR	0.376451876		TMEM241	0.33725352
CD28	0.375479931		LRRC8E	0.33687255
SPN	0.375445685		WWC1	0.33547581
SEPT9	0.375424783		SMPDL3B	0.33257909
VNN1	0.375308908		ATP1A1OS	0.33190942
IL15RA	0.374493716		STXBP2	0.33157797

CYBB	0.374482364		TTC17	0.32945208
KIAA0226L	0.373987455		VAPA	0.32858956
AIF1	0.373902802		LOC10065277	0.32844061
ARHGAP25	0.373594556		ETAA1	0.32835859
PIK3AP1	0.373531849		ATXN10	0.32758509
ICAM1	0.368821189		UBIAD1	0.32730539
CLEC4A	0.368419871		AP1AR	0.32713375
C1orf38	0.36736005		MREG	0.3260403
CCL13	0.366195123		HIVEP3	0.32550202
HLA-DOA	0.366180944		RBBP8,MIR47	0.32521645
SASH3	0.366127528		TFCP2L1	0.32468779
CTSS	0.366114246		SSX2IP	0.32436738
SLA	0.366093376		TMEM125	0.32416448
SELPLG	0.36556177		PKP4	0.32415074
NCKAP1L	0.365170995		ACTR3B	0.3219082
LRRC33	0.36498645		TXLNA	0.32133202
SLC1A3	0.364740734		CHDH	0.32054579
LOC10013095	0.364617786		KIAA1217	0.3201147
FERMT3	0.363971401		C15orf33	0.31981316
CD180	0.363960172		ASB13	0.31976611
PLEKHO2	0.363925484		ZMYM4	0.31881502
CCR2	0.363225511		TFIP11	0.31842123
HLA-DMB	0.363162694		HAT1	0.31839363
PRF1	0.362887082		ADSS	0.31832345
STX11	0.362064655		SEPT9	0.3182576
EVI2B	0.361558768		SERPINA3	0.31825572
SLCO2B1	0.36001578		SRRM1	0.31819552
GVINP1	0.359054733		ZCCHC7	0.31813627
TMEM176B	0.358117579		MAP3K1	0.31775311
FCGR2B	0.358052915		RAPH1	0.31765403
IKZF1	0.357922255		EXOC1	0.31737275
DOCK2	0.357827748		CHMP4C	0.31702855
NCK1	0.357785596		YY1AP1	0.31697119
HCLS1	0.356634188		DSP	0.3166744
HVCN1	0.356311854		C1RL	0.31665547
ACOT9	0.355528408		CLSTN1	0.31611964
APOBEC3C	0.355110246		KCTD1	0.31587618
SLAMF8	0.354911185		GRHL2	0.31570547
TIFAB	0.354891891		SPINT2	0.31569271
OBFC2A	0.354262942		YTHDF2	0.31549248
NCF4	0.354200447		NEBL	0.31541463
LRRC25	0.353175793		ABI1	0.31526413

AMICA1	0.3527306		CHSY1	0.31513791
NCF1	0.352508001		SLC25A17	0.31507351
TMEM173	0.35250537		NUMA1	0.31463971
CD33	0.352321586		CTNNB1	0.31453348
TNFRSF8	0.352183948		CDCP1	0.31406276
TNFRSF1B	0.352074789		ATP1B1	0.3140267
CCND2	0.351879612		PRRG2	0.31373943
LILRB2	0.351870818		SDCCAG8	0.3135241
LOC10050581	0.351787453		STXBP3	0.31342984
CST7	0.351281727		POT1	0.31335114
IL18BP	0.350866653		LDOC1L	0.31322447
TNFRSF9	0.350534942		KIAA1522	0.31318088
INPP5D	0.350350938		USP54	0.31315222
LAIR1	0.350002174		SNRNP40	0.31312131
PSD4	0.349951287		HOOK1	0.31298747
GLIPR1	0.349917104		RSBN1L	0.31270369
SLAMF1	0.349781611		CAMSAP3	0.31267664
RUNX3	0.349694493		WDR35	0.31258713
IL2RA	0.349327653		C1orf109	0.31238441
PIK3CG	0.349259905		KIAA1671	0.31228474
PAQR8	0.348875132		C5orf28	0.31225764
ITGAL	0.348647208		CCDC28A	0.31217149
CLEC4E	0.348548139		SPTBN1	0.31186696
CD68	0.348516826		ARHGEF2	0.31174149
GIMAP1-GIMA	0.348366742		CGNL1	0.31173989
CYTIP	0.348341883		KIAA0040	0.31167894
CLEC10A	0.347943653		KANSL1	0.31154163
CELF2	0.347823599		TBX3	0.31139257
LPXN	0.347723862		USP43	0.31096344
KLHL6	0.347173109		NUP50	0.31087485
CD274	0.346986792		SH2D3A	0.31049164
IL7R	0.346782111		AGPAT5	0.31045971
MDFIC	0.346617351		KIAA0895	0.31038068
BATF3	0.34642437		AP1M2	0.31023572
SIGLEC10	0.345714358		BAIAP2L1	0.31018033
ALOX5AP	0.345650062		SLC11A2	0.31017238
FLI1	0.345226765		ZNF627	0.3098785
SIGLEC5	0.344884822		CAPRIN1	0.30984835
NFAM1	0.344334901		OMA1	0.30979806
EVI2A	0.343913534		HNRNPC	0.30975676
CD200R1	0.343864566		EYA3	0.30969042
AP1S2	0.343713782		CNKSR1	0.30962642

PTPRC	0.343672589		C4orf36	0.30952814
VSIG4	0.343234253		DCAKD	0.30944461
RIN3	0.343210528		CELSR2	0.3094255
C16orf54	0.343105854		SLC25A15	0.30941774
LIMK1	0.3430513		LRRC42	0.30933741
TOR4A	0.342890701		SLC44A1	0.30914657
ACOT7	0.342836082		TMEM63A	0.30899281
CSF2RA	0.342726995		LIMK2	0.30897653
LAX1	0.342703505		MYO6	0.30897184
P2RY13	0.342492571		TMEM154	0.3089383
GLIPR2	0.342459114		ABCD3	0.30852004
SH3KBP1	0.342167149		MYB	0.30827811
MAPRE2	0.342052365		C1orf210	0.30826605
HCK	0.342007337		EIF2A	0.30819988
FGD2	0.341901158		HDAC1	0.30798957
IGFLR1	0.341798659		RBBP4	0.30798201
ICAM3	0.341295317		FBXO3	0.30798175
MNDA	0.341199524		PROM2	0.30783484
FAM49A	0.340983892		ARHGEF5	0.30781867
CCDC82	0.340874113		ASB3,GPR75-	0.30759319
FCN1	0.340667723		PHACTR4	0.30757244
ITGB2	0.340664767		CEACAM1	0.30752034
DNM2	0.34001811		OFD1	0.30749315
C1R	0.339962443		SLMAP	0.30745491
MILR1	0.339668482		MKL1	0.30738049
IFI16	0.33954464		COPG2	0.30729599
IFNAR2	0.338754259		GGA1	0.30728386
PPP1R18	0.338142229		EPHA1	0.30724083
SAMSN1	0.337746186		RAB8A	0.30708488
CXCR6	0.337589277		PRKRA	0.30705745
IRF4	0.337382831		ZZZ3	0.30703983
CD74	0.337080755		PHKA1	0.30701913
CD226	0.336822104		AGAP1	0.30694038
CARD6	0.336610299		SLC35E1	0.30651885
TC2N	0.336379561		RARG	0.30651627
MS4A4A	0.33628115		TCTN2	0.30643613
LILRB3	0.335774588		PTPRF	0.30631817
CHST11	0.335751022		ZNF33A	0.30608727
EVL	0.335668699		ARMCX2	0.30605105
TCN2	0.33561173		SEMA4A	0.30603252
GPR174	0.3355902		ZNF33B	0.30597247
TNFAIP3	0.335395483		JUP	0.30588351

CD163	0.335370036		BRD4	0.30572172
PIK3R5	0.335337072		SPIN1	0.30561736
ACSL4	0.335166384		TRIM44	0.30558867
TLR4	0.335078693		COPG2,TSGA	0.30549601
ETS1	0.334752963		XYLB	0.30545979
CYP7B1	0.33473615		METTL15	0.30537256
SIRPA	0.334363025		MYO5B	0.30536773
C3AR1	0.334251837		ATP1A1	0.30534719
LIX1L	0.334199664		SEMA4B	0.30532774
IL7	0.333909315		PKP3	0.30527969
CPVL	0.333824601		ERBB3	0.30527479
TBX21	0.333431564		FOCAD	0.30520645
NCF1B	0.333384731		PPP1R9A	0.305113
TLR2	0.333381901		CLDN12	0.30506467
LOC283888	0.333374811		NUMB	0.30504264
LYZ	0.333094737		ITGB8	0.30487816
SYT11	0.332945386		CEP70	0.30484084
CD59	0.332936648		DDX17	0.30473986
EMP3	0.332803459		ETV6	0.30472755
MFNG	0.332138679		CASZ1	0.30463407
CMKLR1	0.332099921		DNAJC16	0.30461898
CD300A	0.332005176		NUP35	0.30457237
SLAMF6	0.331985539		CDS1	0.30452827
CD86	0.33190795		KDM3A	0.30450884
MSC	0.331815256		SOGA2	0.30438142
GAB3	0.331621436		RBM47	0.30436077
LGI2	0.331611315		PGM2	0.30429259
BIN2	0.331523214		TMEM168	0.30416005
KCNAB2	0.331503029		SF3A1	0.30413963
GRAP2	0.331494122		PICK1	0.3041336
ANKRD44	0.331109415		CABIN1	0.30406399
CD3G	0.330949053		RPS6KA1	0.30402086
SH2D1A	0.330526096		RSL1D1	0.30398033
FPR1	0.330406483		CHPT1	0.30394407
CRTAM	0.32958559		IL17RB	0.30388839
LILRB1	0.329579574		FAM83F	0.30379925
FYB	0.329375861		KDM1A	0.30374831
TNFSF8	0.329350396		AMBRA1	0.30363002
RASSF4	0.329338392		MAP7	0.30361539
FAM20A	0.329228552		ESRP1	0.30347434
EOMES	0.329096808		SLC25A12	0.3034393
C10orf54	0.329068157		C3orf17	0.30330309

LRMP	0.329056956		ABI2	0.30330103
ELMO1	0.328995544		DSG2	0.30329687
HAPLN3	0.328917596		CXADR	0.30328422
ARHGAP30	0.328708378		HOMER2	0.30328106
WIPF1	0.328505417		IMPACT	0.30310174
IRAK2	0.328099488		SS18	0.30294586
VIM	0.327905213		CELSR1	0.30289381
NKG7	0.327900916		MAP3K9	0.30284879
BTN3A2	0.327737396		C15orf44	0.30283694
LILRB4	0.327711994		OLA1	0.30282821
GZMB	0.327686351		RGNEF	0.30278756
LOC10023320	0.327498536		APP	0.30274939
CD247	0.327226038		RBBP8	0.30266839
JAZF1	0.327137819		ZNF37A	0.30263566
CSF1	0.326787655		L3MBTL2	0.30262954
HLA-DQA1	0.326763391		SIPA1L3	0.30262373
SLAMF7	0.326639321		INADL	0.30257927
FUT4	0.326576855		PRLR	0.30256664
DPYD	0.326543518		AUH	0.30256572
IL21R	0.326255975		DNAL4	0.30255359
ADCY7	0.326218398		API5	0.3025148
PTGER4	0.326172655		PVRL4	0.30247705
GPR65	0.326012801		ZNF791	0.30245145
HLA-DRA	0.3258517		SLC44A3	0.30241609
SLC9A9	0.325556464		GGA2	0.3024102
KLRD1	0.325508103		CSNK1G3	0.30235333
IL10	0.325414342		FBXO30	0.30233912
HLA-DRB5	0.325293165		PON2	0.30231889
HLA-DPB1	0.325225521		SREBF2	0.30231238
GPR183	0.324802824		PPP6R2	0.30230668
PTPN7	0.324714732		DDX31	0.30227548
CD96	0.324688012		DEPDC5	0.30226639
GIMAP1	0.324347638		FHDC1	0.30226313
MS4A6A	0.324330074		PPP4R1	0.30217944
TBXAS1	0.324266997		DYNLT3	0.30215219
AKNA	0.324166671		CHERP	0.30213305
RASSF2	0.323977729		SP3	0.30211538
NCF1C	0.323661897		SFI1	0.3021018
FCGR2A	0.323463935		CRYZ	0.30208222
GIMAP6	0.32338261		RHPN2	0.30206795
GMFG	0.323320513		NMNAT3	0.30202844
PSTPIP1	0.323253895		RAI14	0.30202513

FAM78A	0.323192425		PTBP1	0.30201982
TRAF1	0.323183055		PDLIM5	0.30201237
OPTN	0.323154141		POLDIP3	0.30192907
HAVCR2	0.323002352		ILDR1	0.30190414
TLR6	0.322683525		ERN1	0.30186801
UBASH3B	0.32263836		HEATR1	0.30184776
MYO1G	0.322564273		AGBL5	0.30184351
TNFAIP8L2	0.322443371		ARSD	0.30172685
CHST2	0.322427186		HNRNPU	0.30166651
MYO5A	0.322392769		FAM129B	0.30162326
SIRPB1	0.32237897		EPB41	0.30159408
THEMIS	0.322091821		ZNF317	0.30158835
DSE	0.32159631		SHROOM3	0.30158786
HCST	0.321571689		NDE1	0.30158665
PYHIN1	0.321447675		CASP2	0.30158539
GNG2	0.32134957		REPS1	0.30153321
MARCH1	0.321306739		GPR89A	0.30152674
CORO1A	0.321140438		MORC2	0.30152571
BTK	0.320970912		SND1	0.30145013
IL32	0.320703336		PIGN	0.30139014
AOAH	0.320634821		MLLT4	0.30136548
LAMP3	0.320542771		ZCCHC17	0.3013573
CDKL1	0.320432105		EXOSC10	0.30133504
PHACTR1	0.320413918		CELF1	0.30133493
PARP15	0.320317042		FAM102B	0.30131338
PTPN6	0.320169482		SRSF11	0.30130714
LIPG	0.320134528		KIAA0528	0.30122954
LAPTM5	0.320105723		DDR1	0.30122722
NCF2	0.319922471		DDAH1	0.30116961
CECR1	0.319570397		CD59	0.30115261
ZC3H12D	0.319392014		FAM83H	0.30114991
RNASE6	0.319379424		FARP1	0.301138
FAM20C	0.319257312		ERLEC1	0.30110231
CASP1	0.319256078		EML2	0.30106996
SERPING1	0.31916463		NAV2	0.30102697
STAT5A	0.319071547		ZMYND11	0.30102282
HLA-E	0.319010782		PAK1	0.30100345
PML	0.318954051		LRP2	0.30100021
RGS18	0.318912196		ZC3H7B	0.30097942
LRRFIP2	0.318830205		HPS4	0.30096668
SPOCK2	0.318758908		HNRNPK	0.30090882
GBP1	0.318677835		PUM1	0.3009088

CD84	0.318641348		CYP51A1	0.30088139
SLC2A5	0.318508443		AMFR	0.30087974
MCFD2	0.318414935		BNIPL	0.30087322
GFI1	0.318387274		OSBPL1A	0.30085993
ITK	0.318374188		GRHL1	0.30085988
SBNO2	0.318363822		KCTD3	0.30084376
IL17RA	0.318032615		LYPD6	0.30084187
IL2RB	0.317895714		DLG3	0.3008407
TRPV2	0.317739366		NUP133	0.3008185
CD8A	0.317714557		FBXO7	0.30073647
C1QB	0.317691501		DUSP16	0.30072969
SIGLEC14	0.317276046		ZFAND4	0.30071698
SERPINB9	0.317126427		EIF4ENIF1	0.30065438
SLC8A1	0.317105819		FAM134A	0.30065423
SLA2	0.317104164		GLI3	0.30064457
GBP4	0.316940757		GTPBP1	0.30062736
TUBB6	0.316896169		PAPSS1	0.30061427
CD83	0.3167353		DTNB	0.30060428
FPR3	0.316628328		SPTAN1	0.30059429
PIK3CD	0.316572444		ASH1L	0.30057161
C1QA	0.316515897		EP300	0.30056901
CLIP2	0.316463518		PARN	0.30055252
CTSZ	0.316422632		MACF1	0.30054571
TLR10	0.316307058		DNMT1	0.30047271
SIT1	0.316013028		RABL2B	0.30047168
FCER1G	0.316007767		KDSR	0.30045023
VNN2	0.316005984		SPECC1L	0.30041107
SIPA1	0.315994603		MFSD6	0.30040383
TMEM150B	0.315939328		SPINT1	0.30039395
S1PR4	0.315937551		ARHGEF12	0.30038652
GIMAP4	0.315932838		PTPN9	0.30038153
FMNL1	0.315873263		ATXN7L3	0.30037419
PLA2G2D	0.315778905		FAM198A	0.30035186
SIGLEC7	0.315493144		GPBP1L1	0.30032496
IL18R1	0.315490095		LAMC2	0.30031426
CIITA	0.315457021		PCNXL2	0.30029702
NECAP2	0.315450412		CLUL1	0.30029531
C10orf128	0.31539804		KIAA1191	0.30028818
MPP1	0.315358983		DGCR2	0.30027758
RNF19B	0.315333601		PSD4	0.30027118
IL16	0.31529818		MAGI3	0.30026278
GIMAP7	0.315258043		PIK3CB	0.30025572

OSBPL3	0.315141542		INTS7	0.30024542
TIGIT	0.315009926		MFSD1	0.30020537
PPP1R16B	0.314931933		MICALL1	0.30013156
CD300C	0.314864577		PION	0.30012843
FAM65B	0.31476444		DHX34	0.30011905
IRF8	0.314642035		FLNB	0.3001068
LCP2	0.314591637		TLK1	0.30009122
BCL2A1	0.314527373		PUS7	0.30007213
CR1	0.314467276		COG2	0.30003053
SLC7A7	0.314383927		MARCH8	0.30001073
RCSD1	0.314333478		RNF2	0.3000106
CSDA	0.314254776		PRPS2	0.30000608
SH2D2A	0.314209919		PDE1B	-0.30000886
ABI3	0.31412582		ECHS1	-0.30605585
CCDC50	0.31394181		FTL	-0.30612301
RNF145	0.313872942		SLC2A4RG	-0.30719697
CORO1C	0.313849342		FAM96B	-0.30749696
SPI1	0.31382622		SLC9A3R2	-0.31081107
CTSC	0.313757056		FHOD1	-0.31383827
CCL5	0.313755389		TM7SF2	-0.32011637
CLIC2	0.313677586		PFKFB1	-0.32717401
WDFY4	0.313552766		VAMP5	-0.33155483
CEP85L	0.313500696		AGPAT2	-0.33228669
S1PR2	0.313397803		ACOT8	-0.33926703
SIGLEC9	0.313160787		VEGFB	-0.34921597
UPP1	0.313113599			
ELAC1	0.313062369			
JAK3	0.313005606			
PLCL2	0.312977106			
LGALS2	0.312966938			
RELB	0.312867615			
CCL18	0.312841483			
NAIP	0.312439729			
PDE6G	0.312415801			
MIR155HG	0.312379103			
GRK5	0.312250164			
HABP4	0.312226922			
DENND1C	0.312195083			
PPM1F	0.31218835			
GBP5	0.312184585			
TOX	0.312111842			
LST1	0.312101408			

HAS2	0.312062962
TTC7A	0.311928934
CD72	0.31189729
AIM2	0.311867893
TM6SF1	0.311834494
CD209	0.311762893
LHFPL2	0.311578925
ARRB2	0.311533771
XCL2	0.311520462
TRIM22	0.311455827
CTLA4	0.311399753
C1orf162	0.311370574
RASAL3	0.311339992
ETV5	0.31126299
FAIM3	0.311258446
MRC1	0.311224925
NCOA7	0.311133111
GZMH	0.311124691
IL12RB1	0.310826693
FASLG	0.310724281
BTN3A1	0.310696175
KLRB1	0.310685743
CARD11	0.310553763
C1QC	0.31047685
TFEB	0.310382347
PLAGL1	0.310352435
ST8SIA4	0.310281018
HLA-DRB1	0.31021079
KLRG1	0.310160645
CCR1	0.310144025
RASGRP4	0.310071473
LY9	0.310067113
C1S	0.310027992
STAT4	0.309780933
DPEP2	0.309726471
P2RY8	0.309702126
MGAT1	0.309690495
CD2	0.309663374
SYK	0.309630976
GFPT2	0.309611301
GBGT1	0.309606468
SH2D3C	0.309580324

RASGRP2	0.309463201
LILRA5	0.30940264
P2RX7	0.309332545
DENND3	0.309301724
GNA15	0.309298522
MOB3B	0.309297969
TLR1	0.30901096
CD27	0.308816053
TESPA1	0.308706768
CD3D	0.308669471
COTL1	0.308553008
RPS6KA3	0.308550488
UBASH3A	0.308544295
SEPT1	0.308479855
EMILIN2	0.308432864
PLCG2	0.308310394
CD79B	0.308295922
PRDM8	0.308127205
RASA3	0.308106203
CD1C	0.308070046
RAP1A	0.308057415
CTSB	0.308028564
HK3	0.307999632
CLEC12A	0.307951304
CD37	0.307894189
KLRC4-KLRK1	0.307848286
ADAM28	0.307828509
IL2RG	0.307804204
FAM126A	0.307728255
LAT2	0.307724978
PTGS1	0.307716608
PTGDS	0.307716288
TFEC	0.307404012
FAS	0.307329394
C13orf33	0.307263636
PILRA	0.307253103
POU2F2	0.307132962
LOC100132899	0.307095356
TNFSF13B	0.307044398
ACAP1	0.307034267
C8orf80	0.307030432
TRAT1	0.306977495

GGTA1P	0.30692788
BST1	0.306927801
LCP1	0.306916426
HLA-DQA2	0.30690636
QKI	0.306901073
RAC2	0.306829626
CD40LG	0.30682567
CLEC2B	0.30675117
STK17A	0.306648546
IL6R	0.306565024
CD38	0.30654611
PLEKHO1	0.306543921
RGL1	0.306528734
LSP1	0.306400325
PARVG	0.306372044
EBI3	0.306329603
SLC2A3	0.306310022
FCRL6	0.306269823
FAM171A1	0.306248447
AAED1	0.306208668
PRKCB	0.306177513
PTPN22	0.306076017
SIRPG	0.305901063
MRAS	0.305899201
APOBEC3G	0.305844941
BIRC3	0.305841955
ENO1	0.305808719
GZMA	0.305776336
CMTM7	0.30576387
ITGAX	0.305758112
PRKCA	0.305669402
RAB27A	0.305667235
CPNE8	0.305651269
FCRLA	0.305521983
PLAC8	0.305518445
PIM1	0.305461899
LY96	0.305448185
PDCD1	0.305411676
AKR1B1	0.305382779
PTPRE	0.305370085
IPCEF1	0.305361333
FCGR2C	0.30532901

RASSF5	0.305272896
TLN1	0.305258393
ARHGAP15	0.305242745
ACSL5	0.305220183
C3	0.305213349
VAV1	0.305211053
GPR84	0.305161483
ADAMDEC1	0.305065118
KIFC3	0.305042039
MICALL1	0.304978999
DOCK4	0.304930579
NPL	0.304925509
ZBED2	0.304917674
MYO1F	0.304885651
CHST3	0.304794612
CXCL16	0.30473206
HSD11B1	0.304710398
ARHGAP31	0.304703386
GTDC1	0.304694839
FLJ27354	0.304623725
DUSP7	0.304494941
NCR3	0.304467508
EMR2	0.304421776
C2	0.304421694
CCDC71L	0.304417087
RAB8B	0.304404549
VCAM1	0.304357887
PLEKHG1	0.304289073
SPSB1	0.30423604
BANK1	0.304165693
CCL2	0.30415535
CCR4	0.30409605
ADCY3	0.304068611
CPXM2	0.304005158
NLRC4	0.303962547
STAP1	0.303958367
IL4I1	0.303928375
MEI1	0.303889206
PRKX	0.303749287
SRGAP2	0.303743322
CHI3L1	0.303716725
IGSF6	0.303716638

HLA-DQB1	0.303708036
RND3	0.30369298
APOL6	0.30368597
TCP11L1	0.303677166
ITGAM	0.303650377
PDPN	0.303619781
UNC13D	0.303612764
CD3E	0.303559661
MYO7A	0.303527085
APBB1IP	0.303527075
PNRC1	0.303508532
IL15	0.303506983
SYNE1	0.303504461
GIMAP8	0.303501088
GYPC	0.303425273
MKL1	0.303400629
SAMD4A	0.303390376
SH2B3	0.303317221
GBP2	0.303309857
IGF2BP2	0.303285222
CCDC88A	0.303255854
FOLR2	0.303238832
ARPC2	0.303236014
GPR114	0.303170777
CCL4	0.303161104
NLRP3	0.303121191
EPB41L3	0.303111115
FMNL2	0.303073498
MAP4K1	0.3030681
HLA-DPA1	0.303067964
C11orf75	0.303045131
NFE2L3	0.303042014
MLKL	0.303029407
SELL	0.303011607
DFNA5	0.302922692
CD5	0.302886469
MFHAS1	0.302869699
PRDM1	0.302863122
TRIP10	0.302789885
LILRB5	0.302750963
IFNGR1	0.302734446
POU2AF1	0.302699683

FAT1	0.302696343
RBMS1	0.302686026
LILRA6	0.302681986
HLA-DRB6	0.30264657
CYTH1	0.302575766
PLA2G4A	0.302539861
NLRC3	0.302511821
GIT2	0.302501647
STAMBPL1	0.302425761
FYN	0.30240008
ITM2C	0.302335933
FCRL5	0.302306964
FAM26F	0.302260278
FRMD4A	0.302250393
MYO9B	0.302238831
IL27RA	0.302238763
PLIN2	0.30221633
PSAP	0.302204945
MOXD1	0.302165776
MCOLN2	0.302158509
TMEM140	0.302127767
ADPRH	0.302119269
GPR171	0.302118566
RAB32	0.30208832
IL1RAP	0.302020355
ICOS	0.302002163
TOX2	0.301959506
PPARA	0.301957871
TRPM2	0.301942334
CD6	0.301899538
LCK	0.301890472
CHI3L2	0.301878432
TGFBR2	0.301801388
STK10	0.301786068
OSMR	0.301773102
MALL	0.301755457
HLA-DOB	0.301712744
WARS	0.301671219
CD300LF	0.301599718
CFP	0.301595981
IDO1	0.301595326
P2RX1	0.301578372

SEL1L3	0.301552126
BTN3A3	0.301539705
PLA2G7	0.30153958
RABGAP1L	0.301509501
C14orf49	0.301509175
SP140	0.301488613
TLE4	0.301483476
CLMP	0.301480455
PLS3	0.301434449
GNGT2	0.301400537
C1QTNF1	0.301357817
RAPGEF1	0.301318466
CCDC109B	0.301264737
LGMN	0.301227697
MAP7D3	0.301222891
NT5E	0.301214481
DPP4	0.301204492
PLEKHM2	0.301156748
SUN2	0.30114281
MARCO	0.301139808
ANXA1	0.301136913
MYO1E	0.301132419
FMNL3	0.30112247
ITGB7	0.301112471
KLRK1	0.30109928
NFATC1	0.301094143
ARHGAP22	0.301024767
TIMP2	0.301021124
PLD1	0.301019518
SLC9B2	0.301018007
SLFN11	0.301005579
TRIB2	0.300985829
ANTXR2	0.300983552
RFTN1	0.30096947
PLCB2	0.300913836
PTPRO	0.300890022
HMHA1	0.300877511
PARVB	0.300872073
NRP2	0.300859694
DOCK8	0.300843769
ARHGAP9	0.300839095
TSPAN4	0.300813966

DZIP1	0.300806968
TRAF3IP3	0.300794648
RARRES1	0.30074584
NLRC5	0.300739881
CFLAR	0.300732558
EPB41L2	0.300719986
PRR5L	0.300716921
SAMD3	0.300678831
ITGA4	0.300675531
LPCAT2	0.300672483
SGTB	0.300660092
SLC43A3	0.30062906
AXL	0.300622036
NMT2	0.300596725
HLA-DMA	0.300577967
LTA	0.30056357
SKAP2	0.300561078
MAN2B1	0.300554249
PLTP	0.300539076
FSCN1	0.300497954
REXO2	0.300487861
TCF7	0.300486576
CREM	0.300473636
ZEB2	0.300472913
CD48	0.300465515
CLEC7A	0.300460392
CCDC88B	0.300451901
PRKCQ	0.300447747
RNF166	0.300419618
SLC18B1	0.300404055
TYROBP	0.30037665
CTSW	0.300358648
CXCL1	0.300346621
TMC8	0.300329236
GLS	0.300293425
FLNA	0.300288346
MTHFD1L	0.300275319
MFI2	0.300275133
ALOX5	0.300274703
TGFBI	0.300251436
KIAA1274	0.300251141
MCTP1	0.30023006

ARHGEF6	0.300222378
SCIMP	0.300219943
ITGAE	0.300203023
ALDH1A3	0.300200044
ARNTL2	0.300183827
IFFO1	0.300179479
NLRP1	0.300157996
PAG1	0.300142068
LRRK1	0.300103702
PELI1	0.300093048
APOL3	0.300055879
BTLA	0.30005501
ST3GAL2	0.300051916
PTGIS	0.300036927
DOCK11	0.300034551
LY75-CD302	0.300032131
RASGEF1B	0.300010915
AP1G2	-0.30006238
LINC	-0.30016384
PPDPF	-0.30020125
FKBP3	-0.30023809
C17orf28	-0.30038029
CNTD2	-0.30045538
ATP8B1	-0.30048305
MIPEP	-0.30053746
TTC8	-0.30062884
SLC9A3R2	-0.30074262
ERGIC1	-0.30078056
LMX1B	-0.30092303
PVRL2	-0.30095829
BIK	-0.30115036
KRT8	-0.30132504
TRIM3	-0.30174575
UBE3B	-0.3019779
DOLPP1	-0.302089
ATP5G2	-0.3021019
GOLGA5	-0.30249519
KLHDC9	-0.30256621
PIGM	-0.30259436
SOGA1	-0.30260999
TMEM57	-0.30301737
JKAMP	-0.3032048

ABCC5	-0.30337005
C1orf9	-0.30359706
EXD2	-0.30439136
STRBP	-0.30439472
USP7	-0.30480366
TRPT1	-0.30482328
MRPS36	-0.30492286
PRR15L	-0.30507995
CCDC125	-0.30614705
CCDC87	-0.30615276
EPN3	-0.30668917
STARD10	-0.30740325
MTA3	-0.30772829
TSPAN13	-0.30800447
LOC145837	-0.3089374
FKBP4	-0.30946357
GFM2	-0.31028292
MCF2L	-0.31082892
INO80B-WBP1	-0.31090664
YTHDF1	-0.3112922
TMEM141	-0.31167567
LRBA	-0.31285363
SUOX	-0.31302181
CRNKL1	-0.31371308
RUSC1	-0.3156202
LOC100861400	-0.31564182
ATP6V1G1	-0.31692588
ARID2	-0.31697985
SYNJ2BP-COX	-0.31753248
DNAJC14	-0.31753594
PPP1R10	-0.31845861
ZDHHC16	-0.31870133
CTPS2	-0.3213293
SLC22A5	-0.32287848
ERBB3	-0.32445907
C19orf46	-0.32648274
ESRP2	-0.32806701
COQ6	-0.32814499
KIAA0182	-0.3326765
NFS1	-0.33496386
PDXDC1	-0.33814039
LOC93622	-0.33912921

MNAT1	-0.34054054
IRX5	-0.34054253
COPZ1	-0.34095202
VPS52	-0.34200704
SEC16A	-0.34474532
SLC19A2	-0.34727781
CREB3L4	-0.35176073
SMUG1	-0.37507384
NECAB3	-0.38016844